

Impedance Studies of Thermochemically Activated 316L Stainless Steel

Wen Ching Say¹, Chen Chang Chan¹, Jin Shyong Lin², Chien Chon Chen^{3*}, Alex Fang³, Shih Hsun Chen^{3*}

¹ Department of Materials & Mineral Resources Engineering, National Taipei University of Technology, Taipei 10608, Taiwan; ² Department of Mechanical Engineering, National Chin-Yi University of Technology, Taichung 41170, Taiwan; ³ Department of Energy and Resources, National United University, Miaoli 30063, Taiwan; ⁴ Department of Engineering Technology and Industrial Distribution, Texas A&M University, College Station, Texas 77845, USA.

Received: December 5, 2015 / Accepted: December 15, 2015

Abstract

This study proposed a novel thermochemical activation (TCA) method to modify the surface of 316L stainless steel (SS). At the first stage, phosphate ions were introduced to 316L SS surface by a heat-diffusion process. After rapid quenching into calcium citrate solution, calcium and hydroxide ions were sealed in the TCA compound layer. The TCA and original 316L SS were immersed in Hanks' solution to evaluate their biocompatibility. Electrochemical impedance spectroscopy analysis showed that the surface active compound layer affected the TCA 316L SS, and its total impedances of Bode and Nyquist plots were higher than that of the original ones during immersed in Hank's from 1 to 14 days. After TCA treatment, the corrosion resistance increased greatly, and thus reducing the release of ions from stainless steel, such as Fe, Cr, Ni and Mo. In the Ca- and P-rich areas, the ions were guided to deposit in the Hanks' solution, forming bone-like hydroxyl apatite. The treatment has been proven to reduce the ionic release from 316L SS, which is considered to be a great improvement for implanted alloys.

Keywords: 316 L stainless steel; compound layer; electrochemical impedance spectroscopy; quenching; thermochemical activation.

Introduction

Compared with titanium alloys, stainless steel 316L (316L SS) shows better performance in workability, so it has been widely applied to clinical orthopedics for years on temporary fixation and rectifying devices, such as bone nails, bone plates, dental implants, artificial joints, artificial bone, and vascular stents. However, its biocompatibility of 316L SS is poorer than titanium alloys; thus, the issues resulting from corrosion, allergy and pathological changes would occur after implanted for a long time (Oshida et al., 2005; Morais et al., 1999). Corrosion is mainly related to the material's biocompatibility. It starts to occur once contacting with body fluid, resulting in precipitation of metallic ions and derivatives. The metal corrosion products could cause various allergic and cytotoxic reactions to biological tissues, which limited the usage of 316L SS (Fathi et al., 2003; Ohtsu et al., 2007; Feng et al., 2004; Montanaro et al., 2006; Kobayashi et al., 2007). However, through the surface treatment for metallic implantation, 316L SS's corrosion resistance and biocompatibility could be significantly enhanced (Citeau et al., 2005).

The surface-treated biomaterials (Jiri et al., 2014) could be used to guide bone growth, resulting in improved compactness of bone tissues between the implant and bone and achieving Osseointegration (Olivares et al., 2004; Costa et al., 2000; Bren et al., 2004; Say, 2004; Kobayashi et al., 2007; Prado Da Silva et al., 2001; Wang et al., 2003; Kokubo et al., 1990). There-

* Corresponding authors: chentexas@gmail.com (Chien Chon Chen); brucechen.mse90g@gmail.com (Shih Hsun Chen)

fore, in clinical applications, surface modifications are commonly placed on stainless steel; for example, coating an active compound layer containing hydroxyapatite to enhance the metal biocompatibility (Montanaro et al., 2006; Banczek et al., 2009). This study proposed a novel surface treatment process to modifying the surface of 316L SS, in which the materials were thermochemically converted to active compounds. These compounds contained various ratios of calcium, phosphate, and hydroxide. Electrochemical Impedance Spectroscopy (EIS, Banczek et al., 2009; Shi et al., 2009) was used to study the surface corrosion state in Hanks' solution. It is expected that the properties of implants with treated surface could be enhanced, including their anti-corrosion ability and the multiplication and differentiation of adherent bone cells (Patricia et al., 2014).

Experimental Procedures

A piece of AISI 316L SS plate was cut into a round specimen with a diameter of 16 mm and a thickness of 3 mm. After grinding with silicon carbide (SiC) #1500 grit sandpaper, the specimen was further polished with alumina (Al_2O_3) powders with 0.5 μm grit size. Then it was cleaned in an ultrasonic cleaner filled with 95 vol.% alcohol for 5 min, and dried for the following experiments. The prepared 316L SS material was thermochemically activated in titanium phosphate solution (85 vol.% H_3PO_4 , at 170°C for 5 min) so that the phosphorus and titanium ions could diffuse into the surface, forming a phosphate-containing titanium oxide film. Subsequent quenching treatment was carried out in calcium citrate solution, forming an active compound layer with bone elements, such as calcium, phosphate and oxygen. All specimens were observed via scanning electron microscope (SEM) for their morphology, and energy-dispersive X-ray spectroscopy (EDS) for chemical compositions of films as well. ESCA (Electron Spectroscopy for Chemical Analysis, VG Scientific ESCALAB 250) was used to further show the precise proportional distribution of chemical contents on surfaces. EIS spectra were recorded as cell system immersed in 500 ml Hanks' solution (the solution that was used as a buffer system in cell culture media and aided in maintaining the optimum physiological pH level, roughly at 7.0-7.4, for cellular growth) at 37°C throughout the test. A standard three-electrode system was utilized, where the obtained 316L SS specimens were installed as the working electrode. A platinum plate and SCE (saturated Calomel electrode) were the counter and reference electrodes, respectively. The open-circuit potential with an applied amplitude of 10 mV was measured under a frequency span from 10-1 to 105 Hz by a frequency respond analyzer (Solartron Instrument, model 1287), which was coupled with EG&G Parc potentiostat, model 273A.

Results and Discussion

Figure 1 showed the SEM image and EDS result of chemical compositions for the original 316L SS specimens. The ground surface presented a smooth morphology and the constituent elements included Fe, Ni, Cr, Mo and Mn, the typical compositions of stainless steel, as shown in Figure 1(a) and 1(b), respectively. Comparing with the polished 316L SS, Figure 2(a) reported

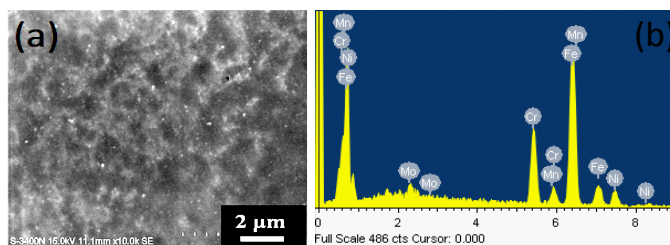


Figure 1. SEM image (a) and EDS result (b) of original 316L SS.

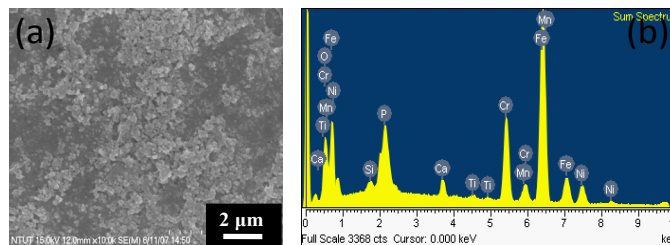


Figure 2. SEM image (a) and EDS result (b) of thermochemically activated (TCA) 316L SS.

that a rough surface coating was formed after TCA treatment. According to the EDS analysis, TCA 316L SS further contained additional elements that were compatible to bone compositions, such as calcium, oxygen and phosphate. This phenomenon proved the surface was changed by the TCA surface treatment, but the practical influenced depth should be further checked. Therefore, ESCA was utilized to detect the depth profiles of thin film's chemical compositions, and the substrate effect could be eliminated due to its controllable incident electron energies. Figure 3 shows a schematic diagram of ESCA element distributed in a compound layer of TCA 316L SS, from 0 nm to 200 nm inside the surface layer. The surface coating was composed of Ca, P, O and Ti, keeping a constant ratio from 0 to 200 nm. Except for Ti, the others are the main compositions of human bones. The Ca/P ratio on the TCA surface was around 1.8, which is close to the theoretic value of hydroxyapatite (HA) (Chang et al., 2002). Thus, TCA treatment deposited a biocompatible coating on the obtained 316L SS.

The results indicated that modifying 316L SS by TCA coating process could effectively allow calcium, phosphorus and other

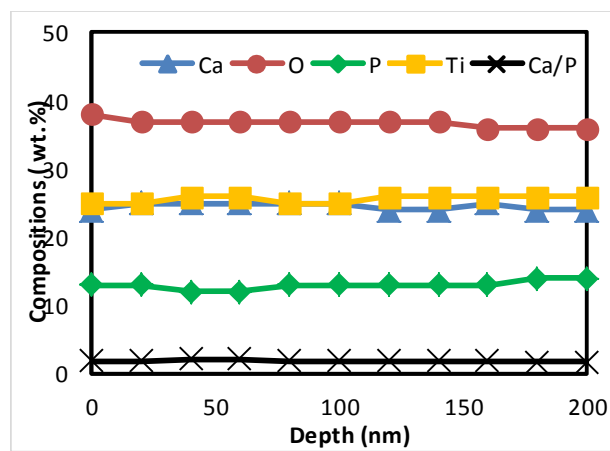


Figure 3. SEM image (a) and EDS result (b) of thermochemically activated (TCA) 316L SS.

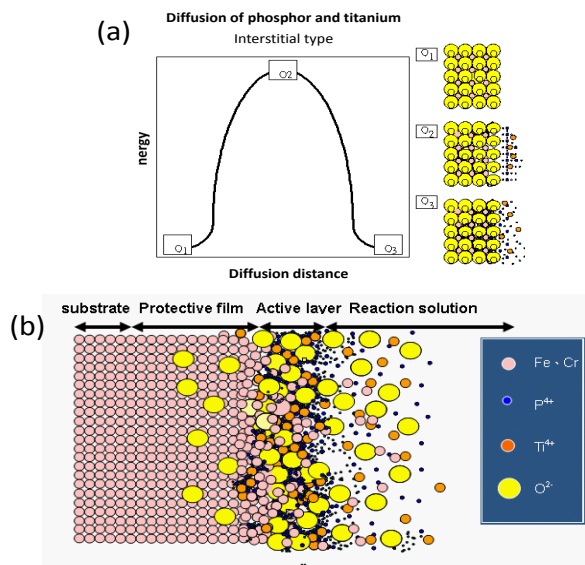


Figure 4. Schematic diagrams of (a) diffusion type and (b) the initial stage of the TCA treatment on 316L SS.

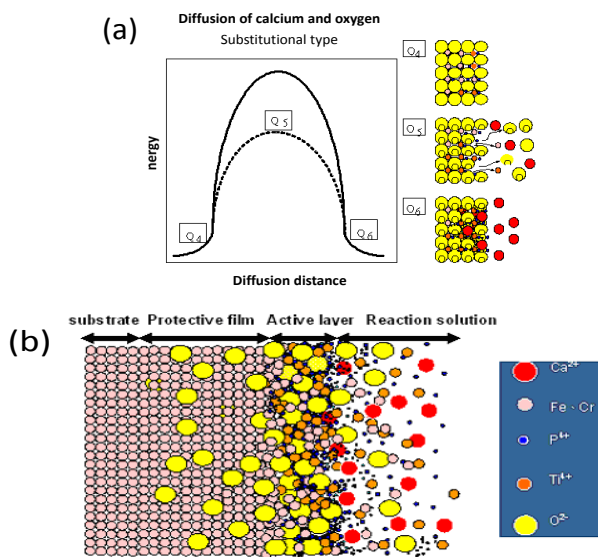


Figure 5. Schematic diagrams of (a) diffusion type and (b) ionic diffusion into 316L SS with TCA surface during quenching in a calcium citrate solution.

elements diffuse into the surface layer, forming a thin film with Ca, P, O and Ti in an activated compound layer with the beneficial Ca/P ratio. Phosphoric acid would easily react with 316L SS and cause chemical conversions with phosphorus ions on the specimen surface. In addition, the activation degree would be accelerated as the acid temperature increased. During TCA process, the phosphoric ions gradually diffused and displaced onto the substrate surface. Figure 4 shows the ionic reaction at the initial stage of the TCA treatment on 316L SS. The schematic drawing in Figure 4(a) describes the three steps of thermal-activated process in phosphoric acid: (i) 316L SS immerses in solution; (ii) phosphoric and titanium ions penetrate through free surface;

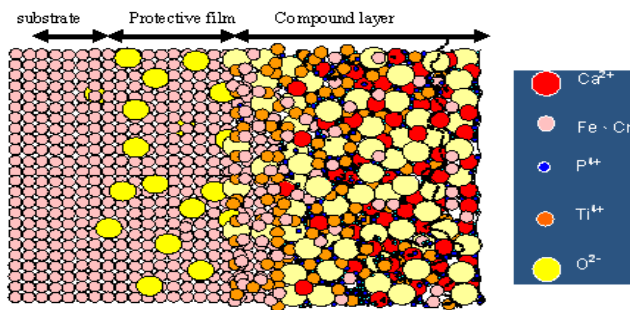


Figure 6. Schematic diagrams of TCA 316L SS.

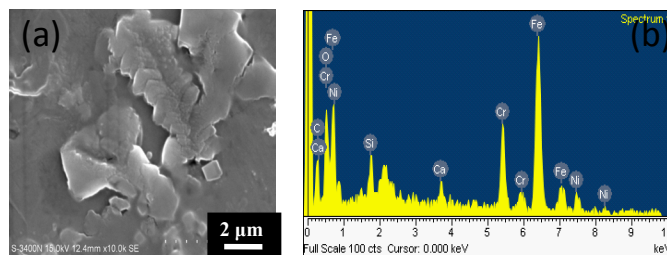


Figure 7. SEM image (a) and EDS result (b) of original 316L SS after immersed in Hanks' solution for 14 days.

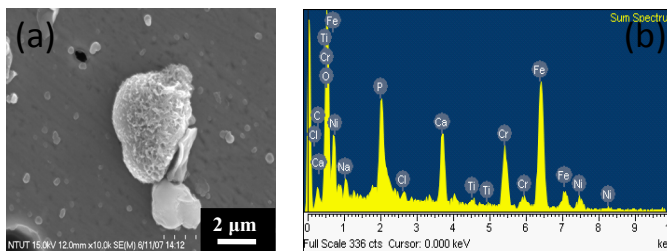


Figure 8. SEM image (a) and EDS result (b) of TCA 316L SS after immersed in Hanks' solution for 14 days.

and (iii) ions diffuse inside 316L SS. This is an interstitial type diffusion reaction, and the energy barrier and diffusion distance to penetrate the surface is the highest. Diffusion mechanism on specimens was also based on the thermal effect from dissociation of phosphoric acid, and then the thermal activated film was quickly quenched and sealed in a calcium citrate solution. As a result, an activated compound layer with strong-bonded bone elements was formed on 316L SS surface. Figure 5 shows the schematic diagrams of ions diffusing at the quenching stage. A series of substitutional reactions occurred when calcium ions contacted the hot phosphatized specimens. TCA 316L SS was obtained after experiencing these two chemical reaction stages. Figure 6 indicates the schematic drawing of the finished TCA 316L SS coating. Furthermore, the original and TCA 316L SS were immersed in Hanks' solution to evaluate their efficiencies on biocompatibility.

Figures 7 and 8 show the SEM images and EDS results for both original and TCA 316L SS, respectively, after immersed in Hank's solution for 14 days. White precipitations on the surfaces were observed, and they were mainly composed of Na, Cl, O, Ca and P. Only TCA specimens showed consistent results with those in past studies (Pereira et al., 1999), in which the bone-like

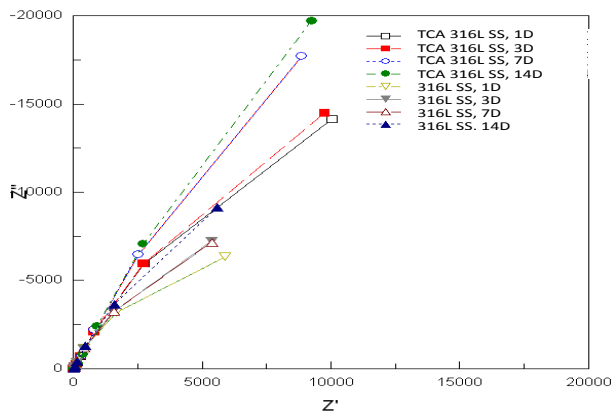


Figure 9. Nyquist diagrams of various 316L SS in Hanks' solution.

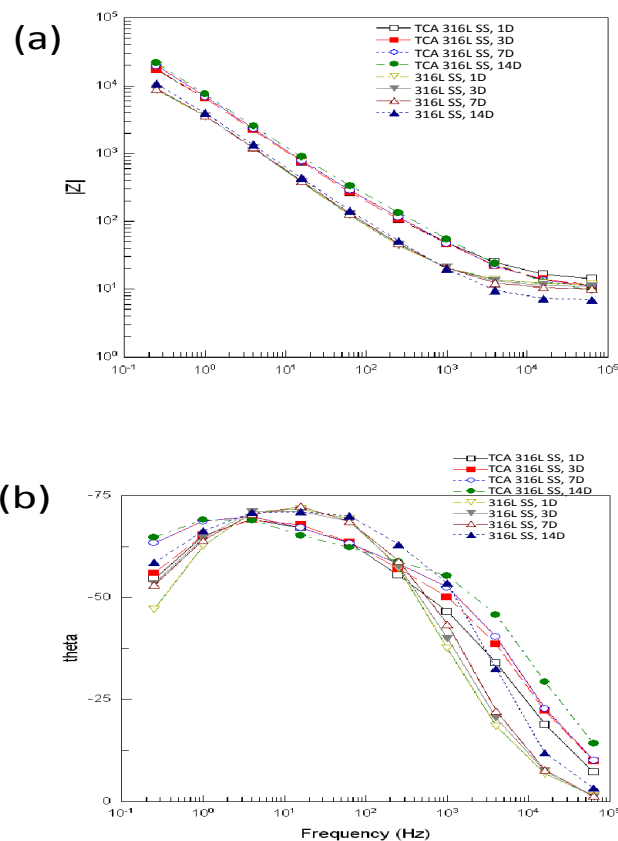


Figure 10. Bode plots of various 316L SS in Hanks' solution. (a) Frequency-impedance plot; (b) frequency-phase plot.

apatite structure was generated on surface containing Ca, P and needle-like crystal. When the immersion time was longer, more bone-like apatite were generated. Thus, the impedance would increase with the immersing time, resulting in enhancing the corrosion resistance of stainless steel (Melissa et al., 1999). In contrast, only calcium salt was detected on the original specimen after immersed for 14 days. Figures 9 and 10 show the impedance changes of specimen immersed in Hanks' solution on the 1st, 3rd, 7th, and 14th days. Therefore, Bode figure presented the relationship between the total impedance and frequency.

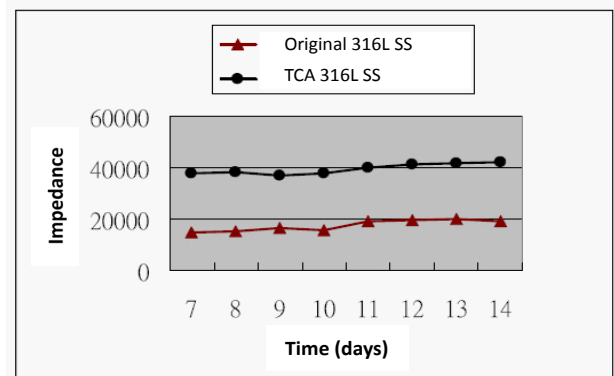


Figure 11. Bode impedance values of various 316L SS after immersed in Hanks' solution from 7 to 14 days.

When the total impedance was higher, it means more calcium salts or thin films of apatite layer were deposited on the surface. The reaction mechanism could be determined by Nyquist plot.

When the radius of the circle was larger, the impedance would be larger. In medium or high frequency, whether after the first day or two weeks, the impedances of the specimen with treated surfaces were all higher than those of the original ones. Since the TCA layer was formed on the surface, the total impedances $|Z|$ of Bode and Nyquist plots increased significantly. Figure 11 shows the total impedances of two specimens immersed in Hanks' solution for 7 to 14 days. According to the comparison of Bode total impedance, the corrosion resistance of the specimen surface with TCA layer was twofold higher than that of the original one. After treatment, the corrosion resistance increased greatly, thus resulting in reduced release of ions in stainless steel, such as Fe, Cr, Ni and Mo. In the concentrated area of Ca and P, the ions can be used to guide the deposition in Hanks' solution, forming bone-like hydroxyl apatite. This result was identical to the findings by Balamurugan et al. (1999). Therefore, TCA treatment could decrease the probability of tissue allergy and inflammation, and thus making the 316L SS implant to be more biocompatible.

Conclusion

The aim of this study was to propose a novel thermochemically activation (TCA) process to modify the 316L SS surface, resulting in a rough surface containing calcium, phosphate and hydroxide ions through thermal diffusion. Characterization of the treated specimens was measured in Hanks' solution for 14 days by using Electrochemical Impedance Spectroscopy (EIS) method. The results of chemical composition analysis indicated that TCA treatment enhanced the attachment of calcium salts and apatite, and TCA 316L SS was coated with a biocompatible thin film.

Acknowledgments

We acknowledge the National Science Council of Taiwan (contracts 103-2221-E-239-004-) for providing the financial support.

References

- Balamurugan A , G Balossier, S Kannan, J Michel, J Faure, and S Rajeswari (2007) Electrochemical and structural characterisation of zirconia reinforced hydroxyapatite bioceramic sol-gel coatings on surgical grade 316L SS for biomedical applications. *Ceram. Inter.* 33: 605-614.
- Banczek EP, LMC Zarpelon, RN Faria, and I Costa (2009) Corrosion resistance and microstructure characterization of rare-earth-transition metal–aluminum–magnesium alloys. *J. Alloys Compd.* 47: 342-347.
- Bren L, L English, J Fogarty, R Policoro, A Zsidi, J Vance, J Drelich, N Istephanous, K Rohly, and J Adhes (2004) Hydrophilic/electron-acceptor surface properties of metallic biomaterials and their effect on osteoblast cell activity. *Sci. Technol.* 18: 1711-1722.
- Chang MC and J Tanaka (2002) FT-IR study for hydroxyapatite/collagen nanocomposite cross-linked by glutaraldehyde. *Biomaterials* 23: 4811-4818.
- Citeau A, J Guicheux, C Vinatier, P Layrolle, TP Nguyen, P Pilet, and G Daculsi (2005) In vitro biological effects of titanium rough surface obtained by calcium phosphate grid blasting. *Biomaterials* 26: 157-165.
- Costa MA and MH Fernandes (2000) Proliferation/differentiation of osteoblastic human alveolar bone cell cultures in the presence of stainless steel corrosion products. *J. Mater. Sci. Mater. Medicine* 11: 141-153.
- Fathi MH, M Salehi , A Saatchi, V Mortazavi, and SB Moosavi (2003) In vitro corrosion behavior of bioceramic, metallic, and bioceramic-metallic coated stainless steel dental implants. *Dent. Mater.* 19: 188-198.
- Feng B, J Weng, BC Yang, SX Qu, and XD Zhang, (2004) Characterization of titanium surfaces with calcium and phosphate and osteoblast adhesion. *Biomaterials* 25: 3421-3428.
- Jiri G, M Holinka, and CS Moucha (2014) Antibacterial Surface Treatment for Orthopaedic Implants. *Int. J. Mol. Sci.* 15: 13849-13880.
- Kobayashi E, M Ando, Y Tsutsumi, H Doi, T Yoneyama, M Kobayashi, and T Hanawa (2007) Inhibition Effect of Zirconium Coating on Calcium Phosphate Precipitation of Titanium to Avoid Assimilation with Bone. *Mater. Trans.* 48: 301-306.
- Kokubo T , S Ito, ZT Huang, T Hayashi, S Sakka, T Kitsugi, and T Yamamuro (1990) Ca,P-rich layer formed on high-strength bioactive glass-ceramic A-W. *J. Biomed. Mater. Res.* 24: 331-343.
- Melissa GS and JB Kirk (1999) Toxicity measurement of orthopedic implant alloy degradation products using a bioluminescent bacterial assay. *J. Biomed. Mater. Res.* 45: 395-403.
- Montanaro L, M Cervellati, D Campoccia, and CR Arciola (2006) Promising in vitro performances of a new nickel-free stainless steel. *J. Mater. Sci.: Mater. Med.* 17: 267-275.
- Morais S, N Dias, JP Sousa, MH Fernandes, and GS Carvalho (1999) In vitro osteoblastic differentiation of human bone marrow cells in the presence of metal ions. *J. Biomed. Mater.* 44: 176-190.
- Ohtsu N, K Sato, K Saito, K Asami, and T Hanawa (2007) Calcium phosphates formation on CaTiO₃ coated titanium. *J. Mater. Sci. Mater. Med.* 18: 1009-1016.
- Olivares R, SE Rodil, and H Arzate (2004) In vitro studies of the biomineralization in amorphous carbon films. *Surf. Coat. Technol.* 177: 758-764.
- Oshida Y, CB Sellers, K Mirza, and F Farzin-Nia (2005) Corrosion of dental metallic materials by dental treatment agents. *Mater. Sci. Eng. C* 25: 343-348.
- Patricia C, ALA Escada, KC Popat, and APRA Claro (2014) Interaction between mesenchymal stem cells and Ti-30Ta alloy after surface treatment. *J. Biomed. Mater. Res.* 102A: 2147-2156.
- Pereira MDC, MDL. Pereira, and JP Sousa (1999) Individual study of chromium in the stainless steel implants degradation: an experimental study in mice. *Biometals* 12: 275-280.
- Prado MH, D Silva, JHC Lima, GA Soares, CN Elias, MCD Andrade, SM Best, and IR Gibson (2001) Transformation of monetite to hydroxyapatite in bioactive coatings on titanium. *Surf. Coat. Technol.* 137: 270-276.
- Say WC (2004) Fabrication of a biomedical implant material with active compound layer on the surface containing calcium, phosphorus and oxygen element. R.O.C. Patent No. 202041.
- Shi P, WF Ng, MH Wong, and FT Cheng (2009) Improvement of corrosion resistance of pure magnesium in Hanks' solution by microarc oxidation with sol-gel TiO₂ sealing. *J. Alloys Compd.* 469: 286-292.
- Wang XX , W Yan, S Hayakawa, K Tsuru, and A Osaka (2003) Apatite deposition on thermally and anodically oxidized titanium surfaces in a simulated body fluid. *Biomaterials* 24: 4631-4637.